Numerical Investigation of the Mixing Mechanism of Passive Micromixer with Tesla Structure

Esra Agel *‡, Batı Altindag **, Osman Ergin ***, Zeynep Kunt**** Ali Bahadir Olcay*****

* Biomaterials, Biomechanics and Bioelectronics Center of Excellence, TUBITAK MRC Gebze-Kocaeli, Türkiye

**BaykarTech, Esenyurt, 34000, Istanbul, Türkiye

***Brunel and Eaton, John M. Keynesplein 33, 1066 EP, Amsterdam, Netherlands

****Ford OTOSAN, Sancaktepe, 34885, Istanbul, Türkiye

*****Yeditepe University, Faculty of Engineering, Department of Mechanical Engineering, Kayisdagi Cad., 34755, Istanbul, Türkiye

(esra.agel@tubitak.gov.tr, batialtindag1998@gmail.com, osmannergin23@gmail.com, zeynep.kunt@std.yeditepe.edu.tr, bahadir.olcay@yeditepe.edu.tr)

‡Esra Agel Tel: +90 262 677 3167, Fax: +90 262 6412309,esra.agel@tubitak.gov.tr

Received: 27.03.2023 Accepted:10.09.2023

Abstract- Passive micromixers using Tesla structures are commonly used in microfluidic systems for efficient fluid mixing. To understand the mixing mechanism of such micromixers, numerical investigations can be performed using computational fluid dynamics (CFD) simulations. In this study, we aimed to improve the mixing mechanism in microfluidic applications using the Tesla valve, which is a static valve that allows the flow of liquids in only one direction. The study analyzed the effect of fluid inlet velocity and surface roughness on the mixing performance of a numerical model. The model was used to test a mixture of water and blood at four flow velocities: 0.15, 0.35, 0.5, and 1.0 m/s. Additionally, the study evaluates the effect of surface roughness on mixing performance by assigning a uniform roughness value of 12 µm to all surfaces in the model. The results showed that fluid mixing primarily occurred in the curved portions of the model, while fluid streams remained separate in the straight segments. There was no backflow, indicating successful fluid transmission without the need for additional valves or switches. The study also includes three cross-sections designated as cross-sections #1, #2, and #3, each at a vertical distance of 0.55 mm, 1.00 mm, and 1.75 mm from the inlet, respectively, to visualize the impact of surface roughness on mixing quantitatively. Overall, the study demonstrated that two Tesla structures can efficiently mix different fluid types, and the Tesla valve is scalable, durable, and easy to fabricate in various materials for microfluidic applications.

Keywords Passive micromixers, microfluidic devices, Tesla valve, surface roughness, fluid mixing.

1. Introduction

Micromixers with Tesla valves are microfluidic devices that use passive valve technology to mix fluids. The Tesla valve is a complex structure consisting of a series of connected chambers with specific geometries that compel fluid to loop back on itself, creating high mixing efficiency. The Coanda effect, which causes fluid to adhere to the surface of the valve, enhances the mixing process, particularly in cases of turbulent flow. Micromixers are microfluidic devices designed to mix multiple fluid streams on a small scale, offering advantages such as high mixing efficiency, fast mixing times, and low fluid consumption. They are widely used in various applications, including chemical synthesis, biochemistry, lab-on-achip systems, medical diagnostics, and point-of-care testing (POCT) devices. [1]. Understanding the fundamentals of fluid flow characteristics in micromixers is vital in determining the structure of the lab on disk systems [2,3]. Fluid mixing in these systems is crucial when different fluids need to be mixed due to fluid density and viscosity differences. While the desired application of these systems can be a washer or a

buffer, working with a system with the least number of moving bodies, such as isolation or regulation valves, is favorable. Therefore, passive micromixers [4] promise to do the job generally without requiring any external effect and making the fluids get mixed with a minimum number of parts using their geometrical shapes solely. Passive mixing in a microchannel has the advantage of higher reliability because there are no moving parts while not requiring additional power and control [5].

Passive micromixers are also known to help fluids mix rapidly while being easily integrable and improving the mixing efficiency at high flow rate values [6]. In 1920, Tesla filed a patent for his "valvular conduit." It resembles a pipe in essence, but one with a complex internal structure that compels fluid to loop back on itself at different points along its length. When water enters the loops' mouths, it becomes agitated, slows down, and stops flowing. However, when water is run oppositely, it bypasses the loops and flows freely [7]. For example, the Tesla valve seems to be a promising model as it is a structure that makes the working mechanism of micromixers more efficient with its simple structure. Besides, the fluid staying attached to the surface, known as the Coanda effect provided by the valve, is effective in highspeed and low-speed mixing, which can benefit the turbulent flow case [8]. Passive micromixers that have the Tesla structures in them are understood to influence the flow with the Coanda effect. There have been considerable amounts of research about passive micromixers with Tesla valves. The main interest is the high mixing efficiency of this type of micromixer. Another essential characteristic of the flow with a Tesla valve system is to have a one-way flow with the least amount of backflow [9]. This characteristic can be quite favourable for a project requiring sensitive motion, such as working with a blood sample for diagnostic purposes.

In the present study, a passive micromixer with two Tesla structures with two different types of fluid and various flow velocity values is numerically investigated to reveal mixing phenomena. The present work focuses on the effect of Tesla structures on the fluids' flows passing through the micromixer. A variety of parameters related to disk is considered to compare the different inlet velocity effects, pressure drops, volume fraction, and streamlines. Lastly, surface roughness occurring inherently during the manufacturing of a micromixer is also evaluated in the study to determine its effect on mixing blood and water fluid streams.

2. Materials-Methods

Understanding the fluid dynamics and mixing in these types of systems can lead to developing a portable system using nanoparticle technologies for on-site diagnosis of infectious agents that can be transmitted through blood (LAB-A-LAMP) project. At the same time, within the scope of the present work, it is aimed to provide information about the behaviour and progress of the flow under the influence of Euler forces without a lab-on-a-disk prototype produced. Passive micromixers can be used in different morphologies. The use of Tesla structures is common, as well as different geometries [10] inspired by Tesla structures. ‘’Figure 1’’ shows a typical Tesla structure and possible upstream fluid directions. Two different fluids coming from two different channels are allowed to mix and follow the downstream channel until they mix and leave the structure from the channel on the right as shown in ‘’Fig.1’’.

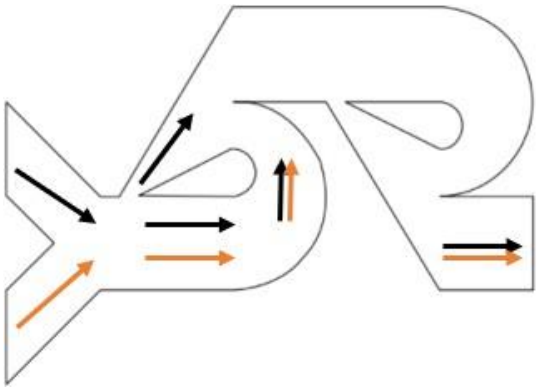

Fig. 1. A passive micromixer [11].

The simulations are carried out as steady and transient for different scenarios in the present study. The steady simulations are chosen to be executed with constant revolutions per minute (RPM) to obtain the numerical results for specific parameters, which will be discussed later. Transient simulations are run to investigate the effect of RPM values on the results where the RPM value is being altered with a ramp-up function.

Reynolds number (Re), used to identify whether a flow is laminar or turbulent, is defined based on fluid velocity, channel width, and fluid's kinematic viscosity. Water properties are obtained from the ANSYS material library, while properties for blood are defined as given in ‘’Table 1’’. As blood shows a Non-Newtonian fluid behaviour, variation of fluid viscosity changing with shear stress, blood viscosity is defined using the Bird-Carreau non-Newtonian model.

Table 1. Analysis reference conditions [12].

Analysis Reference Conditions		
Density	1060	kg/m^3
High Shear Viscosity	0.003 45	Pa.s
Low Shear Viscosity	0.056	Pa.s
Time Constant	3.313	-
Power Law Index	0.356 8	-

The model's geometry is created as a passive micromixer with two-tesla structures using the Design Modeler module of ANSYS 19.2, as shown in ‘’Fig.2a’’ [5]. The approach is to divide the model's inlet face in two to let two different fluids enter the system separately. The mixing of two

different fluids can occur purely because of the geometrical shape of the passive mixer without any need for external effect with this model [13]. As seen in ''Fig.2b'', it is assumed that blood and water come from 2 different reservoirs when determining the boundary conditions. Therefore, the surface of the inlet part is split into two equal parts, and water flows from one part while blood flows from the other. As the outlet condition, gauge pressure is equalized to atmospheric pressure. The output surface has been extended so that the flow in the control volume is not affected by the output boundary condition. Lastly, the wall of the surfaces is defined as a smooth and rough wall in the present study to investigate the effect of roughness on mixing performance.

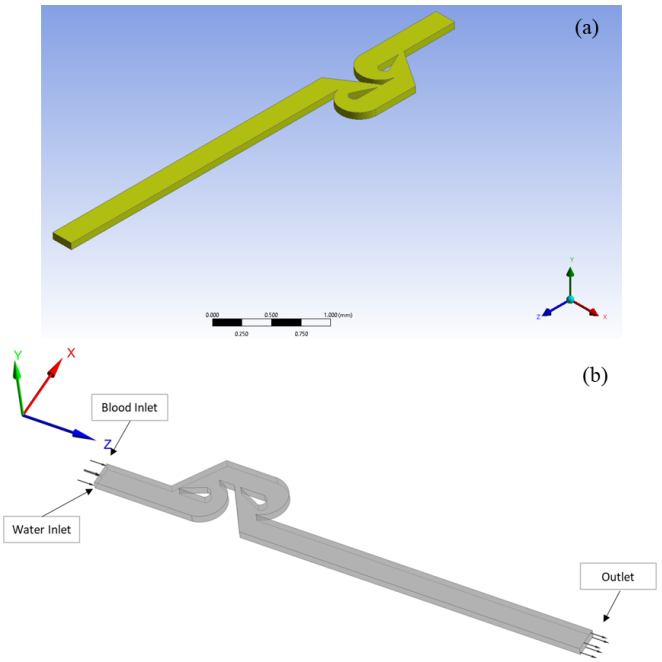

Fig. 2. The geometry of the passive micromixer (a); Boundary conditions for control volume (b).

The geometry's mesh is constructed to maintain a high-quality mesh throughout the entire computational domain. After performing mesh convergence tests, the total number of elements is decided to be over 800 000. Besides, the mesh quality is monitored, and parameters related to mesh quality are provided in ''Table 2''. ''Figure 3'' shows the mesh structure of the computational domain, while an enlarged view of one meshed Tesla structure is given in ''Fig.4''. Furthermore, the computational model is virtually cut into two pieces to illustrate the mesh structure inside the numerical model, as shown in ''Fig.5''.

Table 2. Mesh parameters used in constructing the mesh.

Mesh Parameter	Value
Element Size	0.015 mm
Max Skewness	0.903
Inflation Option	Uniform
Inflation Maximum Layers	20
Inflation Growth Rate	1.2
Total Number of Elements	883746

Fig. 3. Mesh of the whole model.

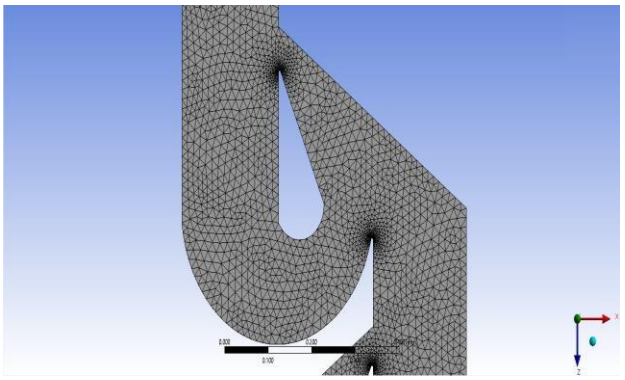

Fig. 4. Mesh of one of the Tesla structure.

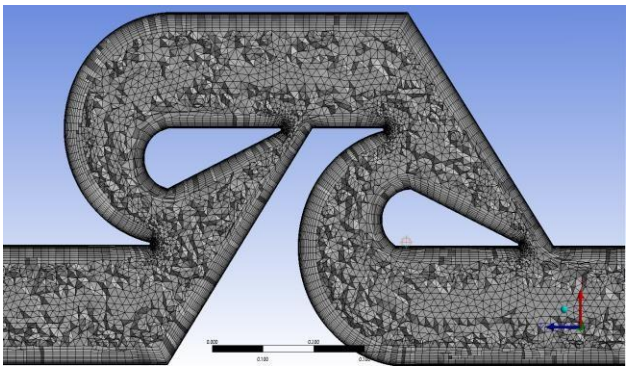

Fig. 5. Cross-section view of the mesh on the model.

Mesh convergence tests allowed us to determine the number of elements required to obtain results independent of the mesh size. Therefore, volume fraction variation is calculated at three different crosssections in the numerical model and monitored during mesh convergence tests, as shown in ''Fig.6''.

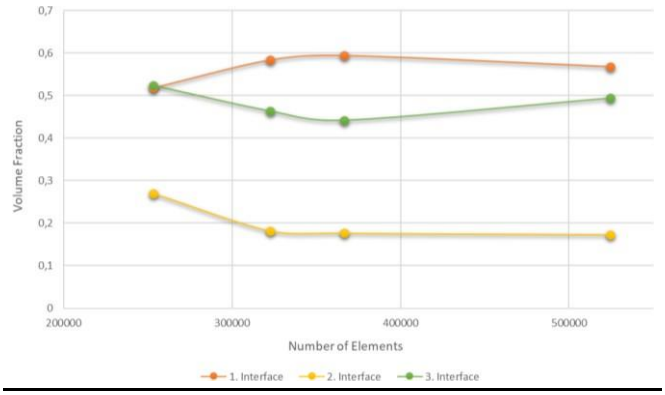

Fig. 6. Volume fraction variation, along with a number of elements used in the convergence tests.

While mesh convergence tests reveal the minimum number of elements needed to obtain accurate results, time-convergence tests provide the largest time step size required to capture important flow parameters such as volume fraction. Time convergence tests results, shown in ''Table 3'', indicate that using 0.1 s as time step size would be sufficient to obtain volume fraction with reasonable accuracy. Therefore, a 0.1 s time step size is chosen for transient simulations, and the total time duration is determined to be 10 seconds, yielding 100 runs for each unsteady fluid flow simulation.

Table 3. The difference in the volume fractions at different time step sizes.

Volume Fractions at Cross Sections			
0.35 [m/s]	Time Step Size [s]		Difference (%)
	0.1	0.01	
CS 1	0.4995	0.4987	-0.2 %
CS 2	0.4194	0.421	0.4 %
CS 3	0.3401	0.3461	1.8 %

3. Results and Discussion

When a passive micromixer inscribed to the disk structure starts to rotate along the disc's center, fluid velocity at the micromixer inlet, the disc's rotational speed, and the Reynolds number vary proportionally as they are all related. Furthermore, the fluid velocity changes in correspondence with the rotation rate of the disc as the centrifugal force exert an effect on the fluid within the inscribed channel. ''Figure 7'' below shows how inlet velocity in the numerical model and Reynolds number vary at different disk speeds expressed as revolutions per minute (RPM). While gray and orange-filled circles present blood and water, blue-filled rectangle shows a fluid mixture. As the disk speed increases, a mixture of blood and water inlet velocities enhance, yielding an increase in the Reynolds number calculated based on water and blood.

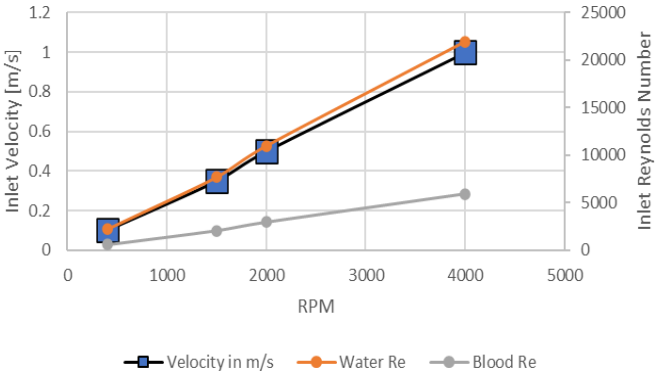

Fig. 7. Inlet velocity and Reynolds number variation with disk speed in RPM.

The present study investigates the effect of flow velocity and surface roughness on mixing efficiency at the computational domain exit by carrying out steady-state simulations. Specifically, a mixture of water and blood at four different flow velocities, 0.15 m/s, 0.35 m/s, 0.5 m/s, and 1.0 m/s, is examined to determine the influence of the fluid inlet velocity on the mixing performance at the exit of the numerical model. Surface roughness, generally responsible for turning the flow regime from laminar to turbulent, is also studied by defining a uniform roughness of 12 μm to all surfaces so that mixing enhancement due to surface roughness can be evaluated. Therefore, Figure 8 below shows fluid flow characteristics results of 0.15 m/s, 0.35 m/s, 0.5 m/s, and 1.0 m/s velocity inlet of passive micromixer numerical models. Besides, simulations are performed in channels with and without roughness, computational models and results are presented in ''Fig.8''.

The first three columns of ''Fig.8'' illustrate pressure, water, and blood velocity contour plots for 0.15, 0.35, 0.50, and 1.0 m/s fluid inlet velocities with and without surface roughness on the inscribed channels, respectively. The pressure drop at low fluid velocities can be nearly twice that of high fluid velocities for surfaces with roughness defined. Both fluids must exceed the pressure created by the nature of the mixer at high rpm due to the Tesla structure [14]. After encountering the Tesla structure, fluids cannot preserve its structure in the laminar region and begin to mix in the first Tesla structure. Blood and water also try to maintain their form at the laminar flow regions (Re < 2300). It is noticed that low-pressure regions are formed in the sharp-turning regions.

The last three columns of ''Fig.8'' illustrate volume fraction, streamline, and volume fraction in cross sections contour plots for 0.15, 0.35, 0.50, and 1.0 m/s fluid inlet velocities with and without surface roughness on the inscribed channels, respectively. As can be seen in the streamline region, fluid regions in the inscribed channel can be identified. Besides, regions where water and blood fluid regions split, and mix can be observed in ''Fig.8''. Mainly, fluid mixing occurs in the turning

regions while fluids flow separately in the straight part of the numerical model. Finally, streamline plots indicate a non-existent backflow; therefore, transmitting the fluid mixture is almost completed successfully without additional valves, switches, or any external force to manipulate the flow. This shows a promising simple but effective solution of Tesla structure to the fluidic channels. As a result, relying on the morphology of the fluid domain consisting of two Tesla structures can yield the mixing of different fluids.

As seen in ‘’Fig.9’’, velocities occur in the W-direction for the flow that normally tries to go in the U-direction since the formed recirculation region (shown in the top right picture of Fig.9) push the flow in the Tesla structure. Because of the velocity gradient, the vorticity forms in the X direction of the fluid shifted to the third dimension, so the mixing quickly occurs in the selected control volume. It is noted that when the fluid mixture approaches the Tesla structure, the blood region dominates a large part of the volume fraction, as illustrated in ‘’Fig.8’’. This could be due to the surface tension of blood since blood is more viscous than water. Besides, the blood acts as an imaginary wall of water in the same region, reducing the flow area seen by the water in the blood interface part, causing the speed of the water to increase slightly [15].

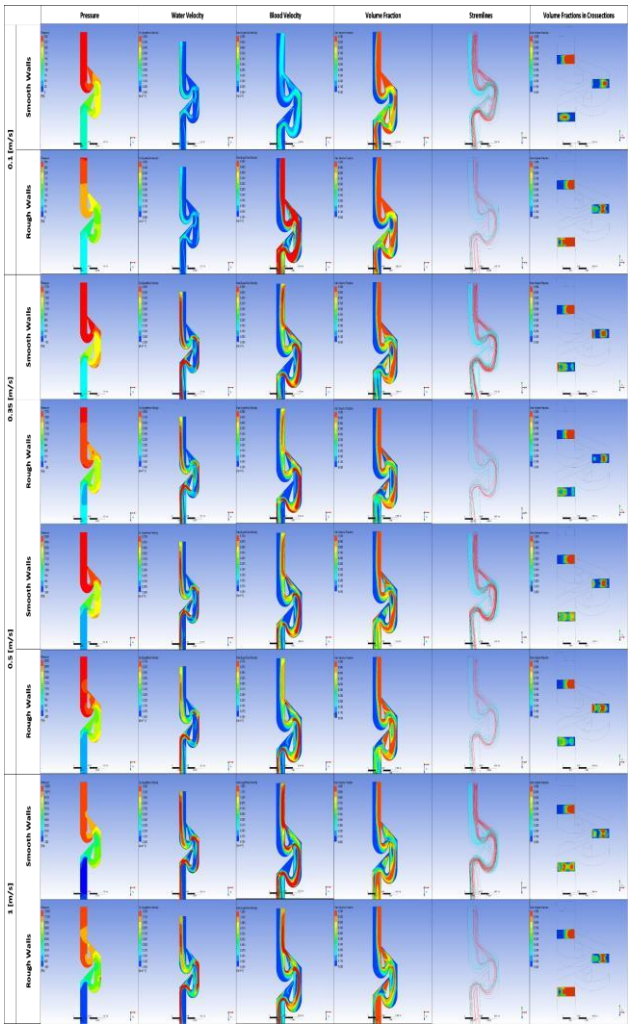

‘’Fig.8’’. pressure (the first column), water velocity (the second column), blood velocity (the third column) contour plots; volume fraction (the fourth column), streamline (the fifth column), and volume fraction (the sixth column) contour plots at different cross sections. Flow velocities of 0.15, 0.35, 0.5, and 1.0 m/s with smooth and rough walls are given from the second to the last row.

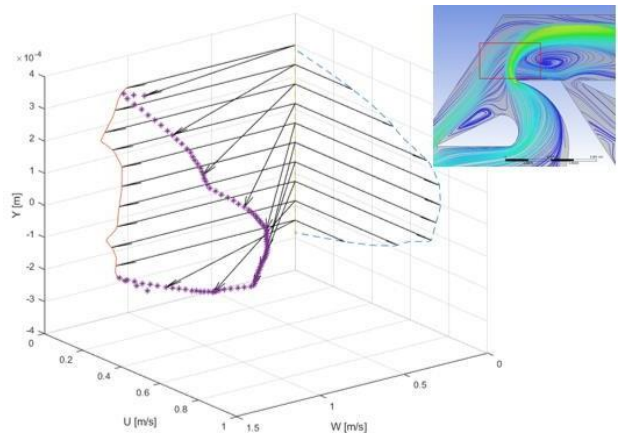

Fig. 9. The crossflow representation of the flow (smooth wall).

Although the numerical model discussed above has smooth surfaces implying no surface roughness, it is not feasible to manufacture a surface without a surface roughness due to limitations in today's manufacturing technologies. The surface roughness on the smooth wall on the Moody chart, used for surface roughness calculations in Fluid Mechanics, was obtained. The flow in the control volume would be highly exposed to wall effects during mixing because of the surface roughness. While the results for the first section were similar to the findings shown in ‘’Fig.11’’, there is a big difference in the results after the fluids entered the Tesla structure. The velocity profiles shown in ‘’Fig.10’’ vary according to the profile in ‘’Fig.9’’ [15]. After the first Tesla structure, mixing occurs differently. For efficient mixing, the volume fraction's value is expected to be 0.5. As a smooth wall, the average value of the volume fractions is likely to be 0.5 compared to the rough walls. The rough walls cause the flow in the disc to slow down around the walls with higher friction caused by more outstanding grip due to greater roughness height. In this case, where the viscous effects increase, the mixture in the structure is adversely affected.

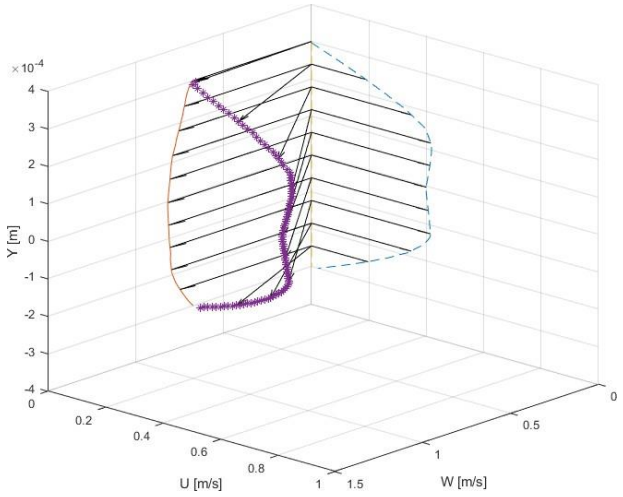

Fig.10. The crossflow representation of the flow (rough wall).

Three different crosssections, crosssections # 1, 2, and 3, with a vertical distance from the inlet of 0.55, 1.00, and 1.75 mm, were created in the numerical model to visualize the effect of surface roughness on mixing quantitatively. Here, volume fraction values of the blood and water mixture for crosssections # 1, 2, and 3 for different inlet velocities are shown in ''Fig.11''. Precisely, the volume of fluid for both smooth and rough wall cases was calculated at those sections to evaluate the mixing behaviour of blood and water, as shown in ''Fig.11''. It is noted that the surface roughness effect appears to be small at the entrance region, as illustrated in ''Fig.11'', while the surface roughness greatly affects volume fraction further down the channel, as shown in crosssections 2 and 3 of ''Fig.11''.

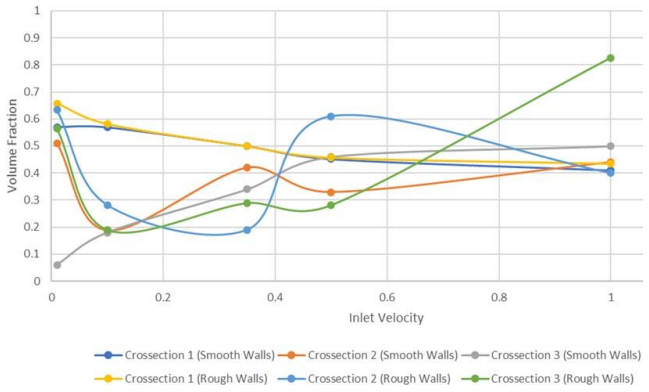

Figure 11. Volume fractions for crosssections # 1, 2, and 3 for different inlet velocities**.**

As the numerical disc model accelerates from 0 RPM and reaches the desired RPM value, the variation of inlet velocity from the beginning is assumed to be linear, as shown in ''Fig.12''. More specifically, to see the effect of the RPM change on the disc, the inlet velocity increases with the RPM value varying from 1500 RPM to 4000 RPM (Figure 7) [10]. Therefore, velocity is defined as a linear ramp function, the input made in Ansys CFX-Pre with a command generating the desired ramp function, as shown in ''Fig.12''. As mentioned in the time convergence section, the mesh results, not much affected by the time step, are shown in ''Fig.13'' for the time step size of 0.1s.

The variation in volume fraction for crosssections # 1, 2, and 3 are also monitored with provided inlet velocity function. There is no significant change in the area-averaged volume fraction results for the first cross-section. However, the volume fraction values in crosssections # 2 and 3 approach 0.5, indicating a perfect mix. As a result, increasing the RPM value seems to increase the efficiency of the mixture for both cross sections #1 and 2.

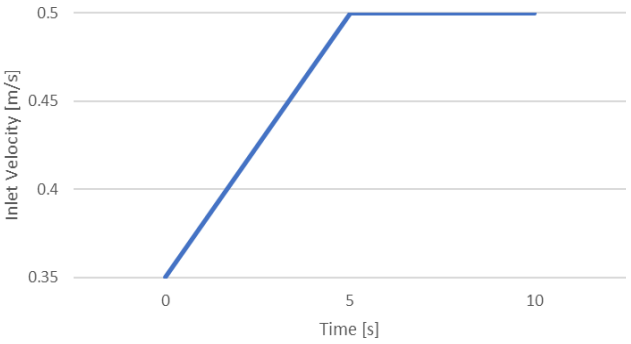

Fig. 12. Inlet velocity function.

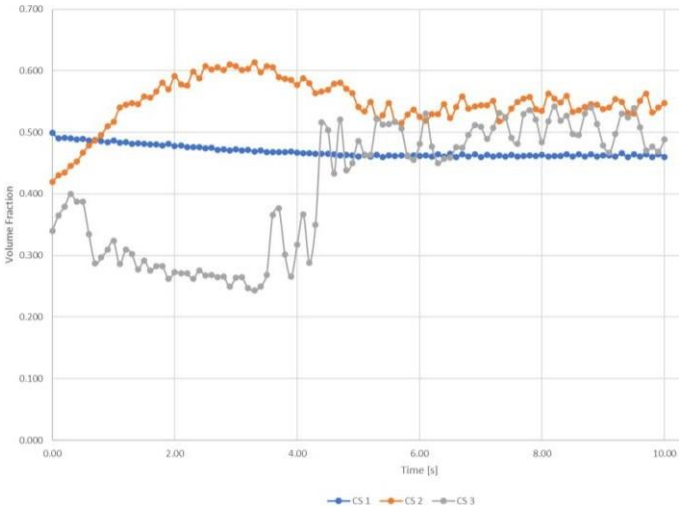

Fig. 13. Variation of volume fractions of crosssections # 1, 2, and 3 at different times.

4. Future work

In the lab-on-a-disc stages, it is seen that blood samples are washed and decomposed at different stages. During this washing or separation, homogeneous mixing of the washing liquid and the sampled blood or other liquid will increase the interaction. High mixing efficiency can be achieved quickly by combining experimental methods with the results obtained with CFD methods, yielding the samples' results to be obtained earlier [16] [17].

The present study shows that using Tesla structures in the design of microfluidic devices can effectively mix fluids

since fluid streams can benefit from Coriolis effects induced by the disc's angular velocities. In addition, with the Coanda effect included in the Tesla structure, at least one of the desired liquids in the mixture is separated at an early stage. Depending on the application, a fluid stream can move together with the other fluid stream separated with the help of geometry merges immediately after the Tesla structure, causing liquids to mix easier. At the same time, these currents induced by the Coriolis effect are further disturbed within geometry. As a result, Tesla structures give promising findings in mixing fluids, and with the addition of different structures, the system's mixing efficiency can be even better [18].

5. Conclusion

Microfluidic devices are miniature systems for handling and manipulating small volumes of fluid, usually in the microliter or nanoliter range. They are used in a wide range of applications, including biochemistry, chemical synthesis, drug discovery, blood sample measurements, and lab-on-a-chip systems. Microfluidic devices offer advantages such as improved reaction kinetics, reduced fluid waste, increased sensitivity, efficient mixing mechanisms, and the ability to handle small samples.

Using Tesla's structure in a numerical micromixer model enabled us to understand how blood and water fluid streams mix. Water and blood velocities and pressure along the micromixer were identified, while volume fraction values at three different cross sections were evaluated to determine the effect of inlet velocity and surface roughness on fluid mixing. The turbulent flow was achieved in the lab on a disc [19] mechanism, including the Tesla structures [20] [21]. Blood and water flow contour is investigated by inserting the interfaces into the Tesla structures; more frequent liquid mixing is observed at the interfaces as it approaches the outlet. As the inlet velocities are increased, the mixing rate increases. In addition, the difference between smooth and rough walls widens, and the flow character changes [22]. Vortices indicate the transitional change from laminar to turbulent [23] [24] at the upstream of the numerical model. Meanwhile, the volume fraction, which serves as a measure of the degree of mixing, commences at approximately half its value at the beginning of the analysis. Subsequently, there is a significant divergence in its value towards the middle of the analysis, before eventually converging and re-establishing balance towards the end of the analysis."

In conclusion, the numerical investigation of microfluidic devices has played a critical role in advancing our understanding of microscale fluid dynamics and its applications. By leveraging mathematical models and computational tools, researchers have been able to study the behaviour of fluid streams and their mixing mechanism in microfluidic systems with unprecedented accuracy and detail. The continued advancement of numerical methods and computational resources is likely to expand the capabilities of microfluidics further and open up new avenues of research in this rapidly evolving field.

Acknowledgment
This research was supported by TUBITAK (The Scientific and Technological Research Council of Türkiye) under Project 1004 Integrated, Scalable, Functional Nanostructures and Systems 20AG004, entitled "Development of a portable system using nanoparticle technologies for on-site diagnosis of infectious agents that can be transmitted through blood (LAB-A-LAMP)."

References

[1] R. Gorkin, J. Park, J. Siegrist, M. Amasia, B. S. Lee, J. M. Park, J. Kim, H. Kim, M. Madou, Y. K. Cho, “Centrifugal microfluidics for biomedical applications”, Lab on a Chip, DOI:10.1039/b924109d, Vol. 10, No. 14, pp. 1758-73, 2010.

[2] C. K. Dixit, A. Kaushik, Microfluidics for biologists: Fundamentals and applications, Microfluid Biol Fundam Appl.,DOI:10.1007/978-3-319-40036-5,Springer International Publishing, pp.1–252.

[3] J. F. C. Loo, H. C. Kwok, C. C. H. Leung, S. Y. Wu, I. L. G. Law, Y. K. Cheung, Y. Y. Cheung, M. L. Chin, P. Kwan, M. Hui, S. K. Kong, and H. P. Ho, “Sample-to-answer on molecular diagnosis of bacterial infection using integrated lab--on--a--disc.”, Biosensors & bioelectronics, 93, 212–219, 2017. DOI:10.1016/j.bios.2016.09.001.

[4] M. Bayareh, M. N. Ashani, A. Usefian, "Active and passive micromixers: A comprehensive review", Chem Eng Process - Process Intensif 2020;147:107771. DOI: 10.1016/j.cep.2019.107771, Vol.147, pp.1-42.

[5] C. C. Hong, J. W. Choi, C. H. Ahn, “A novel in-plane passive microfluidic mixer with modified Tesla structures”, Lab Chip, DOI:10.1039/b305892a, Vol.4, pp. 109-113.

[6] C. T. Wang, Y. M. Chen, P. A. Hong, Y. T. Wang, "Tesla valves in Micromixers", Int J Chem React Eng., DOI:/10.1515/ijcre-2013-0106, Vol. 12, pp. 397-403.

[7] A. A. Yontar, D. Sofuoğlu, H. Değirmenci, Ş. Biçer, T. Ayaz, “Investigation of Flow Characteristics for a Multi-Stage Tesla Valve At Laminar and Turbulent Flow Conditions”, Journal of Scientific Reports-A, Vol.47, pp. 47–67.

[8] C. C. Hong, J. Choi, C. H. Ahn, “A Novel In-Plane Passive Micromixer Using Coanda Effect”, Micro Total Analysis Systems, pp. 31-33.

[9] N. Tesla. Valvular conduit (U.S. Patent No. 1, 329,559) 1920.

[10] S. Ranković, B. Bojović, “An example of passive micromixer design, simulation and optimization”, 2015 4th Mediterranean Conference on Embedded Computing (MECO), DOI:10.1109/MECO.2015.7181953, IEEE publishing, pp. 395-398, 2015.

[11] I. Stanciu, “Uncertainty analysis of mixing efficiency variation in passive micromixers due to geometric

Tolerances", Model Simul Eng., DOI:10.1155/2015/343087, Vol. 2015, pp.1-8.

[12] O. Mutlu, A. B. Olcay, C. Bilgin, B. Hakyemez, "Evaluating the Effect of the Number of Wire of Flow Diverter Stents on the Nonstagnated Region Formation in an Aneurysm Sac Using Lagrangian Coherent Structure and Hyperbolic Time Analysis", World Neurosurg DOI:10.1016/j.wneu.2019.09.116, 133:e666–82.

[13] X. Wang, L. Yang, F. Sun., "CFD analysis and RSM optimization of obstacle layout in Tesla micromixer", Int J Chem React Eng,, DOI: 10.1515/ijcre-2021-0087, pp. 1-11.

[14] M. Madou, J. Zoval, G. Jia, H. Kido, J. Kim, N. Kim, "Lab on a CD", Annu Rev Biomed Eng, DOI: 10.1146/annurev.bioeng.8.061505.095758, Vol. 8, pp. 601-628.

[15] A. Butler, X. Wu, "Non-Parallel-Flow Effects on Stationary Crossflow Vortices at Their Genesis", Procedia IUTAM, DOI: 10.1016/j.piutam.2015.03.055, Vol.14, pp. 311-320.

[16] A. Purwidyantri, B. A. Prabowo, "Tesla Valve Microfluidics: The Rise of Forgotten Technology", Chemosensors, DOI: 10.3390/chemosensors11040256, Vol.11, pp.1-22.

[17] T. Q. Truong, N. T. Nguyen, "Simulation and optimization of Tesla valves", 2003 Nanotechnol Conf Trade Show - Nanotech, Vol.1, pp. 178–181, 2003.

[18] F. Schönfeld, V. Hessel, C. Hofmann, "An optimised split-and-recombine micro-mixer with uniform chaotic mixing", Lab Chip, DOI:10.1039/b310802c.,Vol.4, pp. 65–69.

[19] M. Itoh, Y. Yamada, S. Imao, M. Gonda, "Experiments on turbulent flow due to an enclosed rotating disk", Exp Therm Fluid Sci, DOI:10.1016/0894-1777(92)90081-F, Vol. 5, pp. 359-368.

[20] X. Chen, Z. Zhao, "Numerical investigation on layout optimization of obstacles in a three-dimensional passive micromixer", Anal Chim Acta, DOI:10.1016/j.aca.2017.01.066, Vol.964, pp. 142-149.

[21] M. B. Habhab, T. Ismail, J. F. Lo, "A laminar flow-based microfluidic tesla pump via lithography enabled 3D printing", Sensors, DOI:10.3390/s16111970, Vo. 16, pp. 1-10.

[22] L. Guo, H. Xu, L. Gong, "Influence of wall roughness models on fluid flow and heat transfer in microchannels", Appl Therm Eng, DOI: 10.1016/j.applthermaleng. 2015.04.001, Vol.84, pp.399–408.

[23] M. A. Faruque, R. Balachandar, "Seepage effects on turbulence characteristics in an open channel flow", Can J Civ Eng, DOI:10.1139/L11-041, Vol. 38, pp. 785–799.

[24] J. Yang, N. Francois, H. Punzmann, M. Shats, H. Xia, "Diffusion of ellipsoids in laboratory two-dimensional turbulent flow", Phys Fluids, DOI: 10.1063/1.5113734, Vol.31, pp.1-8.